Published in final edited form as:
J Hepatol. 2007 July ; 47(1): 103–113. doi:10.1016/j.jhep.2007.02.024.

Gliotoxin causes apoptosis and necrosis of rat Kupffer cells *in vitro* and *in vivo* in the absence of oxidative stress: Exacerbation by caspase and serine protease inhibition

Kristin Anselmi, **Donna B. Stolz**, **Michael Nalesnik**, **Simon C. Watkins**, **Ravindra Kamath**, and **Chandrashekhar R. Gandhi**
Thomas E. Starzl Transplantation Institute, Departments of Surgery, Cell Biology and Pathology and VA medical Center, University of Pittsburgh, Pittsburgh, PA, USA

Abstract

Background/Aims—A potential application of gliotoxin therapy for liver fibrosis was suggested by its apoptotic effect on fibrogenic activated stellate cells. We investigated if gliotoxin exerts similar effects on hepatic macrophages Kupffer cells.

Methods—Effects of gliotoxin on Kupffer cells isolated from the normal liver and *in vivo* following its administration to CCl_4–induced cirrhotic rats were studied.

Results—Gliotoxin caused apoptosis of cultured Kupffer cells, the effect being apparent at 0.3 μM concentration within 1 hour; longer incubation caused necrosis. This effect was associated with mitochondroial cytochrome c release, caspase-3 activation and ATP depletion. Interestingly, inhibition of caspase-3 and serine proteases accelerated and augmented gliotoxin-induced cell death via necrosis. Gliotoxin stimulated nuclear translocation of NFκB, and phosphorylation of p38, ERK1/2 and JNK MAP kinases, but these signaling molecules were not involved in gliotoxin-induced death of Kupffer cells. *In vivo* administration of gliotoxin to cirrhotic rats caused apoptosis of Kupffer cells, stellate cells and hepatocytes. In control rats, the effect was minimal on the nonparenchymal cells and not apparent on hepatocytes.

Conclusions—In the fibrotic liver, gliotoxin nonspecifically causes death of hepatic cell types. Modification of gliotoxin molecule may be necessary for selective targeting and elimination of activated stellate cells.

Keywords

Apoptosis; Fibrosis; Gliotoxin; Kupffer cells; Liver; Necrosis; Stellate cells

INTRODUCTION

Gliotoxin, a fungal metabolite, belongs to the epipolythiodioxopiperazine class of compounds. Gliotoxin (0.3–7.5 μM) was reported to cause apoptosis of activated rat and human hepatic stellate cells (HSCs) by inducing mitochondrial permeability, cytochrome c release and

Correspondence to: Chandrashekhar R. Gandhi, Ph.D, Thomas E. Starzl Transplantation Institute, University of Pittsburgh, E-1518 BST, 200 Lothrop street, Pittsburgh, PA 15213, Phone: (412) 648-9316; Fax: (412) 624-6666, gandhics@upmc.edu.

caspase-3 activation (1,2); higher concentrations (>7.5 μM) caused necrosis of activated human HSCs in association with increased oxidative stress (2). These were important observations as activated HSCs play a central role in liver fibrosis and sinusoidal component of portal hypertension (3). HSCs produce several growth factors, cytokines and chemokines (4,5) responsible for initiation and progression of liver pathology. Therefore, strategies to remove selectively activated HSCs from the fibrotic liver are intensely investigated.

Gliotoxin possesses immunomodulating activity: it stimulates lymphocyte proliferation, and induces T cell cytotoxicity and lymphokine release by T cells (6–9). Gliotoxin (10–100 nM) was found to inhibit phagocytic activity of peritoneal and circulating macrophages (6,7,9) at concentrations lower than those required to cause apoptosis of HSCs. High concentration of gliotoxin (>1 μM) induces reactive oxygen species (ROS)-mediated apoptosis of peritoneal macrophages, independent of the inhibition of phagocytosis (8). The role of hepatic macrophages Kupffer cells extends from defense against invading microbes and clearance of toxic substances to liver growth and immune regulation (10–13). These functions of Kupffer cells are even more critical in disease states as their removal can significantly augment pathological development (14). Since gliotoxin-induced elimination of activated HSCs could be therapeutic strategy for liver fibrosis, it is important to rule out its adverse effects on other hepatic cell types. Therefore, we investigated the effects of gliotoxin on rat Kupffer cells *in vitro*, and in control and CCl_4-induced cirrhotic rats *in vivo*.

MATERIALS AND METHODS

Gliotoxin, TPCK, MG132 (Sigma, St. Louis, MO); PD98059, SB203580, SP600125 and PDTC (Calbiochem, La Jolla, CA); Z-DEVD-fmk (R&D, Minneapolis, MN); Mn-TBAP (Calbiochem, La Jolla, CA); anti-rabbit NFκB-p65, ERK1/2 and caspase-3, mouse anti-rat desmin antibodies and CY-3-conjugated goat anti-rabbit secondary antibody (Santa Cruz Biotechnology, Santa Cruz, CA); anti-rabbit monoclonalP-ERK1/2, P-p38, p38, P-JNK and JNK antibodies (Cell Signaling, Danvers, MA); anti-rat ED2 antibody (Serotech, Raleigh, NC); peroxidase-linked anti-rabbit IgG (Amersham-Pharmacia, Piscataway, NJ) were purchased.

Isolation and culture of Kupffer cells and activated stellate cells

IACUC, University of Pittsburgh approved the protocols in accordance with the NIH guidelines. Kupffer cells, prepared essentially as described previously (15), were suspended in William's medium E containing 10% fetal calf serum and plated at a density of 0.5×10^6/cm^2. Medium was renewed after 3h and following day; cells were used on the third day. Purity as determined by immunostaining for ED2 (Kupffer cells), desmin (stellate cells) and SE-1 (endothelial cells) was greater than 95%. Rat liver-derived HSCs were activated in culture and used in passage 3–5 as describe previously (16).

Determination of cell viability and apoptosis

Cell viability was determined by MTT assay as described (16). To determine apoptosis, the cells were washed with PBS, fixed in 4% parafarmaldehyde and incubated with 5 μg/ml propidium iodide at room temperature for 5 min. Morphological evaluation of propidium iodide-stained nuclei was performed by excitation at 380 nm and emission at 520 nm (17). For DNA fragmentation analysis, attached, loosely attached and detached cells were pooled. Total DNA was extracted and following electrophoretic separation (16), ethidium bromide-stained DNA bands were visualized under UV light.

Determination of LDH, ATP, trypan blue exclusion, cytochome c and caspase-3 activity

LDH release and cellular ATP were measured using LDH Liqui-UV Kit [Stanbio Labs (2940-430)] and Cell Viability Assay Kit-ATP (Dojindo Molecular Technologies,

Gaithersburg, MD) respectively. For additional determination of membrane damage, cells from the culture supernatant were pelleted by centrifugation, and the attached cells were trypsinized and washed. The two fractions were pooled, suspended in culture medium and mixed with trypan blue. Trypan blue-positive and negative cells were counted.

Quantikine murine immunoassay kit (R&D, Minneapolis, MN) and caspase fluorescent assay kit (BD Biosciences-Clonetech, San Jose, CA) respectively were used to measure cytosolic cytochrome c and Caspase-3-like activity.

Western blot analysis

Western analysis for caspase-3 and MAPKs was performed as described previously (18).

Determination of NFκB

Immunohistochemical determination of NFκB (18) and gel-shift analysis to demonstrate NFκB-DNA binding (19) were performed essentially as described.

Measurement of superoxide and H_2O_2

The cells were washed and loaded with 10 μm hydroethidine ($O_2\cdot^-$) or dihydro-2′7′-dichlorofluorescein diacetate (H_2O_2) for 30 min at 37°C (20,21). After washing, the cells were treated with gliotoxin, collected by trypisization, and washed with PBS. Fluorescence was measured by flow cytometry within 30 minutes in a Coulter Epics XL Flow Cytometer.

In vivo treatment with gliotoxin

Cirrhosis was induced in male Sprague-Dawley rats by 8 weeks of CCl_4/phenobarbital treatment as described (22). Gliotoxin (3 mg/kg) was administered intraperitoneally 24h after the last CCl_4 injection. The liver was excised 6h later, rinsed with cold PBS, cut into approximately 1 cm^3 pieces, fixed in 4% paraformaldehyde for 2h, placed in 30% sucrose for 16–24h and frozen in 2-methylbutane cooled with liquid nitrogen. Cryostat sections (5 μm) were cut, washed with PBS, incubated in TUNEL reagents (Roche) (30 min; 37°C), followed by streptavidin CY3 (30 min; 22°C). After blocking in 2% BSA solution, sections were incubated with primary antibodies (1:200 in BSA solution) followed by Cy3-conjugated secondary antibody (Jackson Laboratories), then treated with Hoechst dye (1 mg/100 ml), coverslipped with Gelvatol, and analyzed under Olympus BX51 fluorescence microscope.

Statistical analysis

Statistical significance between the groups was determined by one-way ANOVA followed by a test for linear trend. A P value of <0.05 was considered statistically significant.

RESULTS

Gliotoxin decreases Kupffer cell viability

Viability of control cells did not change over 24h (Figure 1A). Gliotoxin (0.03 μM) caused significant reduction in viability only at 24h. At 0.3 μM and 3.0 μM, gliotoxin caused time-dependent loss of viability that was significant at 3h and 1h respectively (Figure 1A); incubation beyond 3h at both concentrations caused detachment of the majority of cells. Gliotoxin caused equivalent loss of viability of Kupffer cells even in the presence of serum (Figure 1B). Pancreatic elastase (apoptotic agent for Kupffer cells) (23) reduced the viability moderately, while necrosis-inducing chlorpromazine (1), caused profound loss of viability (Figure 1B).

Gliotoxin causes apoptosis and necrosis of Kupffer cells

We determined if apoptosis is a mechanism of gliotoxin-induced reduced viability of Kupffer cells. Apoptotic cells increased progressively upon treatment with 0.03 to 3 μM gliotoxin (Figure 2A and 2B). DNA fragmentation analysis confirmed substantial genomic DNA damage at 3h of incubation with gliotoxin (Figure 2C). Incubation for 4h with elastase caused very mild DNA fragmentation; gliotoxin treatment of activated HSCs showed classical DNA fragmentation (Figure 2D).

ATP content did not decrease significantly with 0.03 μM gliotoxin (Figure 3A). However, 0.3 μM gliotoxin caused rapid and progressive decrease in ATP that was profound between 3 and 6h. Robust ATP depletion occurred in cells treated with 3 μM gliotoxin even at 30 min. ATP decreased by about 20% compared to control upon 4h elastase treatment, and could not be detected in chlorpromazine-treated cells at 3h (not shown).

Profound apoptosis and ATP depletion lead to secondary necrosis characterized by membrane damage, LDH release and trypan blue uptake. The time-course and concentration-dependence experiment showed no LDH release at low concentration of gliotoxin (0.03 μM) (Figure 3B). At 0.3 μM gliotoxin, no LDH release occurred at 3h (Figure 3B) although decreased viability and DNA fragmentation was noted (Figures 1 and 2); LDH release occurred at 4.5h, and was maximal at 6h of incubation. At 3 μM gliotoxin, LDH release occurred earlier (at 3h) and was maximal at 6–12h. Chlorpromazine caused LDH release equivalent of that in cells treated with 3 μM gliotoxin and elastase did not exert any effect (not shown).

No difference in the number of cells taking up trypan blue was observed between control and 0.03 μM gliotoxin-treated cells (Figure 3C). Progressive increase in trypan blue uptake was caused by 0.3 μM gliotoxin after 3h. These results suggest that gliotoxin-induced apoptosis (before 3h) precedes cell membrane damage (LDH release and trypan blue uptake after 3h). Treatment with elastase and chlorpromazine for 3h caused trypan blue uptake by 8 ± 3 and 93 ± 7% Kupffer cells. Significant increase in trypan blue uptake was observed in cells treated with 3 μM gliotoxin only for 1h. Thus at high concentration, necrosis seems to be the predominant mode of gliotoxin-induced death of Kupffer cells.

Gliotoxin causes cytochrome c release and caspase-3 activation

Gliotoxin-induced apoptosis of activated HSCs is associated with increased mitochondrial permeability suggesting the release of cytochrome c (24), a caspase-3 activator (25). In gliotoxin-treated Kupffer cells, cytochrome c release occurred at 15 min and progressively thereafter (Figure 4A). Caspase-3 activity, as determined enzymatically, increased time-dependently from 15 min (Figure 4B). However, cleavage of caspase-3 into the active form was observed at 2 and 3h by Western analysis (Figure 4C).

To determine the role of caspases in gliotoxin-induced apoptosis, the cells were preincubated with caspase inhibitor Z-DEVD.fmk. Surprisingly, Z-DEVD.fmk augmented gliotoxin-induced death of the Kupffer cells (Figure 5); a serine protease inhibitor TPCK also exacerbated gliotoxin-induced death of Kupffer cells. Because such effects of these inhibitors were unexpected, we determined if the inhibition diverts the death pathway to necrosis. Indeed, Z-DEVD.fmk exacerbated gliotoxin-induced LDH release and trypan blue uptake by Kupffer cells (Figure 6). Interestingly, TPCK pretreatment caused profound LDH release and trypan blue uptake by gliotoxin-treated cells even at 1h. At 6h, gliotoxin itself caused robust LDH release and trypan blue uptake by Kupffer cells.

Gliotoxin induces MAPK signaling pathways

Several mechanisms of eukaryotic cell regulation involve signal transduction via mitogen-activated protein kinases (MAPK) such as extracellular signal-regulated protein kinases 1/2 (ERK1/2), p38, and the c-Jun NH2-terminal kinase/stress-activated protein kinases (JNK/SAPK) (26–29). To explore the possibility of the role of MAPK in gliotoxin-induced death of Kupffer cells, activation of p-38, JNK and ERK1/2 was determined. Gliotoxin caused activation of all 3 MAPKs with earliest increase in phosphorylation of p38 occurring at 15 min and of JNK and ERK at 30 min (Figure 7A). However, pretreatment with specific MAPK inhibitors prior to the addition of 0.3 μM gliotoxin was found not to affect gliotoxin-induced death of Kupffer cells (Figure 7B).

Gliotoxin causes nuclear translocation of NFκB

Nuclear translocation of NFκB is important in cellular signaling associated with inflammatory stimuli and cell survival. We hypothesized that constitutive activation of NFκB may be inhibited by gliotoxin as in HSCs (1). However, gliotoxin actually stimulated nuclear translocation of NFκB as determined by immunohistochemistry (Figure 8A) as well as by gel shift analysis (Figure 8B). Even at 3h, when the cells were shrunk indicative of apoptosis, strong immunolabeling for nuclear NFκB was seen. In gel shift analysis the specificity of gliotoxin effect was demonstrated by its inhibition with MG132.

Gliotoxin does not induce oxidative stress

In Kupffer cells, gliotoxin did not stimulate SO or H_2O_2 production (Figure 9A, 9B), which are shown to cause DNA damage and death of several cell types (30–32). Moreover, antioxidants PDTC, Mn-TBAP, vitamin E and N-acetylcysteine did not affect gliotoxin-induced decrease in Kupffer cell viability (Figure 10).

In vivo effect of gliotoxin on Kupffer cells

Administration of gliotoxin to rats causes apoptosis of activated HSCs in the fibrotic liver, but not of quiescent HSCs in control liver (1). Considering the strong apoptosis/necrosis of gliotoxin-treated Kupffer cells *in vitro*, we investigated effect of gliotoxin on Kupffer cells *in vivo*. As shown in Figure 11A, glotoxin did not affect viability of hepatocytes in the control liver. Although few apoptotic hepatocytes were observed in DMSO-treated cirrhotic liver (not shown), morphological analysis revealed greater number of apoptotic hepatocytes in gliotoxin-treated cirrhotic liver (Figure 11D). TUNEL staining also showed several apoptotic hepatocytes in gliotoxin-treated fibrotic (Figure 11E, F), but not in the normal liver (Figures 11B, C). Consistent with a previous report (1), apoptotic HSCs were found in gliotoxin-treated fibrotic liver (Figure 11E). Several apoptotic Kupffer cells were also found to undergo apoptosis in the fibrotic liver after gliotoxin administration (Figure 11F). In control rats, gliotoxin caused minimal apoptosis of HSCs and Kupffer cells (<0.01%) (Figure 11B, C). The numbers of apoptotic hepatocytes, HSCs and Kupffer cells in gliotoxin-treated cirrhotic liver were 8 ± 2%, 45 ± 9% and 53 ± 12% respectively.

The above results demonstrated that gliotoxin causes death of Kupffer cells activated *in vivo*. Although activation of cultured Kupffer cells upon short-term treatment with endotoxin (33) did not sensitize them to gliotoxin up to 0.03 μM concentration, further reduction in their viability occurred at 0.3 and 3.0 μM concentration (Figure 12).

DISCUSSION

Here we report that gliotoxin causes death of cultured Kupffer cells via apoptosis and secondary necrosis. Previously, activated rat and human HSCs were found to undergo apoptosis and

exclude trypan blue at 0.3–7.5 μM gliotoxin (1,2) but necrosis was observed at concentration above 7.5 μM (2). Hepatocytes are resistant to lower gliotoxin concentration but undergo necrosis at high concentration (50 μM). Apoptosis of Kupffer cells by lower concentration of gliotoxin (0.03–0.3 μM) indicates their greater sensitivity than HSCs and hepatocytes, and also peritoneal macrophages, which undergo apoptosis at higher (1 μM) concentration (9).

Gliotoxin-induced apoptosis of Kupffer cells involved classical apoptotic pathway of mitochondrial cytochrome c release, caspase-3 activation and ATP depletion. ATP is required for apoptosis but its depletion below a threshold concentration leads to secondary necrosis (34,35). Thus profound loss of ATP might be a mechanism of secondary necrosis of Kupffer cells at later times during gliotoxin treatment. Curiously, although gliotoxin stimulated caspace-3 activation, its inhibition exacerbated gliotoxoin-induced death of Kupffer cells. This finding contrasts the blockade of gliotoxin-induced nucleosomal ladder formation (but not morphological changes) in activated HSCs by caspase inhibitor Z-VAD.fmk (1). In addition, serine protease inhibition by TPCK also exacerbated, even more strongly, the effect of gliotoxin. These unusual and unexpected findings do not have definitive explanation. It is likely that inhibition of caspase-3 activation or serine proteases may promote another pathway (necrotic) of gliotoxin-induced death. Indeed, preincubation of the cells with Z-DEVD.fmk or TPCK caused strong early increase in LDH release and uptake of trypan blue upon gliotoxin challenge.

We investigated the involvement of NFκB, MAPKs and ROS in gliotoxin-induced death of Kupffer cells. Gliotoxin inhibits TNF-α-inducible nuclear binding of NFκB but not constitutively activated NFκB in activated HSCs and promotes apoptosis (1), probably by inhibiting TNF-α-induced activation of antiapoptotic genes (36–39). In contrast, PDTC, an inhibitor of NFκB activation (40,41) and an antioxidant (42,43), blocked gliotoxin-induced death of activated HSCs (1). Since NFκB promotes cell survival, its nuclear translocation by gliotoxin suggested adaptive stimulation of survival pathway, leading to the hypothesis that its inhibition should augment the toxic effect of gliotoxin. However, inability of PDTC to affect gliotoxin-induced death of Kupffer cells indicates that NFκB activation may not be related to this phenomenon or that the overwhelming activation of pro-death mechanisms overrides them. Interestingly, NFκB activation was shown to mediate elastase-induced apoptosis of Kupffer cells (23).

Most evidence indicates that p38 MAPK inhibits cell proliferation (44,45) and promotes apoptosis (46–48); its activation was also shown to be associated with $GdCl_3$-induced apoptosis of Kupffer cells (49). Activation of JNK was found to be associated with apoptosis, presumably by phosphorylation of antiapoptotic Bcl2 members (29,48). There is also evidence for the role of ERK activation in apoptosis (50). However, inhibition of these MAPK pathways did not prevent or inhibit gliotoxin-induced Kupffer cell death suggesting that their activation may be related to other responses.

Gliotoxin-induced apoptosis of peritoneal macrophages was reported to involve ROS (8). Although 1.5–7.5 μM gliotoxin was found to cause apoptosis of culture-activated and immortalized HSCs respectively in the absence or at low level of oxidative stress (2,24), higher concentrations induce oxidative stress and necrotic death of the immortalized HSCs (2). Necrosis of hepatocytes induced by high concentrations of gliotoxin (>10 μM) was prevented by antioxidants catalase and superoxide dismutase (24). However, gliotoxin did not stimulate SO and H_2O_2 generation in Kupffer cells, and several antioxidants did not prevent gliotoxin-induced death of these cells. Together, these observations indicate that the mechanism of gliotoxin-induced death of Kupffer cells(apoptotic and necrotic) is different from that for peritoneal macrophages and HSCs with respect to NFκB or ROS involvement, and is independent of MAPK activation.

Gliotoxin caused apoptosis of Kupffer cells as well as HSCs in the fibrotic rat liver; the effect was minimal in the normal liver. This may be because activated Kupffer cells and HSCs are more sensitive to gliotoxin, and the numbers of both cell types increase in cirrhosis (51). The profound effect of gliotoxin observed on Kupffer cells isolated from normal liver as compared to the minimal effect *in vivo* is interesting. A plausible explanation is that Kupffer cells may be activated in culture similar to those *in vivo* during hepatic injury (52,53). However, the activation does not seem to be complete as preincubation of the cells with endotoxin further sensitized Kupffer cells to gliotoxin-induced death. These observations contrast a recent study reporting comparable gliotoxin-induced apoptosis of Kupffer cells and HSCs in normal and cirrhotic livers (54). The reason for this discrepancy may be that liver slices were incubated for 8h with gliotoxin *in vitro* (54), while we and others (1,24) investigated the effect of gliotoxin *in vivo*. We also found significant gliotoxin-induced apoptosis of hepatocytes in the fibrotic liver but not the normal liver. Since hepatocytes undergo necrosis, but not apoptosis, upon treatment with high (>10 μM) concentration of gliotoxin *in vitro* (1,24), these results suggest that hepatocytes are either modified during fibrosis to become sensitive to pro-apoptotic effect of gliotoxin or that gliotoxin may release proapoptotic stimuli from nonparenchymal cells that then cause apoptosis of hepatocytes.

In summary, our results show that gliotoxin is a nonspecific pro-death agent for HSCs, Kupffer cells and hepatocytes in the fibrotic liver. The results also demonstrate a novel death-augmenting effect (via necrosis) of caspase-3 and serine protease inhibition on gliotoxin-induced apoptosis of Kupffer cells. Considering the importance of macrophages in resolution of fibrosis (55), removal of Kupffer cells might delay this process or even adversely affect the liver. Further research to investigate whether specific derivatives of gliotoxin cause apoptosis of activated HSCs selectively, excluding other liver cell types, is necessary for clinical application.

Acknowledgments

This work was supported by two grants from National Institutes of Health: RO1-DK54401 to CRG and CA76541 to DBS. We thank Dr. C. Thirunavukkarasu for assistance with apoptotic assays and Mr. Mark Ross for immunostaining of liver sections.

Abbreviations

DMSO
: dimethylsulfoxide

HBSS
: Hank’s balanced salt solution

Mn-TBAP
: manganese (III) tetrakis (benzoic acid) porphyrin chloride

PDTC
: pyrrolidine dithiocarbamate

ROS
: reactive oxygen species

TPCK
: tosyl-phenylalanine chloromethylketone

References

1. Wright MC, Issa R, Smart DE, Trim N, Murray GI, Primrose JN, et al. Gliotoxin stimulates the apoptosis of human and rat hepatic stellate cells and enhances the resolution of liver fibrosis in rats. Gastroenterology 2001;121:685–698. [PubMed: 11522753]
2. Kweon YO, Paik YH, Schnabl B, Qian T, Lemasters JJ, Brenner DA. Gliotoxin-mediated apoptosis of activated human hepatic stellate cells. J Hepatol 2003;39:38–46. [PubMed: 12821042]
3. Friedman SL. Molecular regulation of hepatic fibrosis, an integrated cellular response to tissue injury. J Biol Chem 2000 Jan 28;275(4):2247–50. [PubMed: 10644669]
4. Pinzani M, Marra F. Cytokine receptors and signaling in hepatic stellate cells. Semin Liver Dis 2001;21:397–416. [PubMed: 11586468]
5. Maher JJ. Interactions between hepatic stellate cells and the immune system. Semin Liver Dis 2001;21:417–426. [PubMed: 11586469]
6. Mullbacher A, Eichner RD. Immunosuppression in vitro by a metabolite of a human pathogenic fungus. Proc Natl Acad Sci U S A 1984;81:3835–3837. [PubMed: 6203127]
7. Mullbacher A, Waring P, Eichner RD. Identification of an agent in cultures of Aspergillus fumigatus displaying anti-phagocytic and immunomodulating activity in vitro. J Gen Microbiol 1985;131:1251–1258. [PubMed: 2410548]
8. Waring P, Eichner RD, Mullbacher A. The chemistry and biology of the immunomodulating agent gliotoxin and related epipolythiodioxopiperazines. Med Res Rev 1988;8:499–524. [PubMed: 2461498]
9. Eichner RD, Al Salami M, Wood PR, Mullbacher A. The effect of gliotoxin upon macrophage function. Int J Immunopharmacol 1986;8:789–97. [PubMed: 2430903]
10. Naito M, Hasegawa G, Ebe Y, Yamamoto T. Differentiation and function of Kupffer cells. Med Electron Microsc 2004;37:16–28. [PubMed: 15057601]
11. Wheeler MD. Endotoxin and Kupffer cell activation in alcoholic liver disease. Alcohol Res Health 2003;27:300–306. [PubMed: 15540801]
12. Everett ML, Collins BH, Parker W. Kupffer cells: another player in liver tolerance induction. Liver Transpl 2003;9:498–499. [PubMed: 12740793]
13. van der Bij GJ, Oosterling SJ, Meijer S, Beelen RH, van Egmond M. Therapeutic potential of Kupffer cells in prevention of liver metastases outgrowth. Immunobiology 2005;210:259–265. [PubMed: 16164033]
14. Roggin KK, Papa EF, Kurkchubasche AG, Tracy TF Jr. Kupffer cell inactivation delays repair in a rat model of reversible biliary obstruction. J Surg Res 2000 May 15;90(2):166–73. [PubMed: 10792959]
15. Gandhi CR, Hanahan DJ, Olson MS. Two distinct pathways of platelet-activating factor-induced hydrolysis of phosphoinositides in primary cultures of rat Kupffer cells. J Biol Chem 1990;265:18234–18241. [PubMed: 2170406]
16. Thirunavukkarasu C, Watkins S, Harvey SAK, Gandhi CR. Superoxide-induced apoptosis of activated rat hepatic stellate cells. J Hepatol 2004;41:567–575. [PubMed: 15464236]
17. Nicoletti I, Migliorati G, Pagliacci MC, Grignani F, Riccardi C. A rapid and simple method for measuring thymocyte apoptosis by propidium iodide staining and flow cytometry. J Immunol Methods 1991 Jun 3;139(2):271–9. [PubMed: 1710634]
18. Thirunavukkarasu C, Watkins S, Gandhi CR. Mechanisms of endotoxin-induced nitric oxide, interleukin-6 and tumor necrosis factor-a production in activated rat hepatic stellate cells: role of p38MAPK. Hepatology 2006;44:389–398. [PubMed: 16871588]
19. Ganster RW, Taylor BS, Shao L, Geller DA. Complex regulation of human inducible nitric oxide synthase gene transcription by Stat 1 and NF-kappa B. Proc Natl Acad Sci U S A 2001;98:8638–8643. [PubMed: 11438703]
20. Rothe G, Valet G. Flow cytometric analysis of respiratory burst activity in phagocytes with hydroethidine and 2′,7′-dichlorofluorescin. J Leukocyte Biol 1990;47:440–448. [PubMed: 2159514]
21. Narayanan PK, Goodwin EH, Lehnert BE. Alpha particles initiate biological production of superoxide anions and hydrogen peroxide in human cells. Cancer Res 1997;57:3963–3971. [PubMed: 9307280]

22. Gandhi CR, Nemoto EM, Watkins SC, Subbotin VM. An endothelin receptor antagonist TAK-044 ameliorates carbon tetrachloride-induced acute liver injury and portal hypertension in rats. Liver 1998;18:39–48. [PubMed: 9548266]

23. Peng Y, Gallagher SF, Haines K, Baksh K, Murr MM. Nuclear factor-kappaB mediates Kupffer cell apoptosis through transcriptional activation of Fas/FasL. J Surg Res 2006;130:58–65. [PubMed: 16154149]

24. Orr JG, Leel V, Cameron GA, Marek CJ, Haughton EL, Elrick LJ, et al. Mechanism of action of the antifibrogenic compound gliotoxin in rat liver cells. Hepatology 2004;40:232–242. [PubMed: 15239107]

25. Bortner CD, Cidlowski JA. Cellular mechanisms for the repression of apoptosis. Annu Rev Pharmacol Toxicol 2002;42:259–281. [PubMed: 11807173]

26. Sanchez I, Hughes RT, Mayer BJ, Yee K, Woodgett JR, Avruch J, et al. Role of SAPK/ERK kinase-1 in the stress-activated pathway regulating transcription factor c-Jun. Nature 1994;372(6508):794–8. [PubMed: 7997269]

27. Pombo CM, Bonventre JV, Avruch J, Woodgett JR, Kyriakis JM, Force T. The stress-activated protein kinases are major c-Jun amino-terminal kinases activated by ischemia and reperfusion. J Biol Chem 1994;269:26546–26551. [PubMed: 7929379]

28. Bogoyevitch MA, Gillespie-Brown J, Ketterman AJ, Fuller SJ, Ben-Levy R, Ashworth A, et al. Stimulation of the stress-activated mitogen-activated protein kinase subfamilies in perfused heart. p38/RK mitogen-activated protein kinases and c-Jun N-terminal kinases are activated by ischemia/reperfusion. Circ Res 1996;79:162–173. [PubMed: 8755992]

29. Kyriakis JM, Banerjee P, Nikolakaki E, Dai T, Rubie EA, Ahmad MF, et al. The stress-activated protein kinase subfamily of c-Jun kinases. Nature 1994;369:156–160. [PubMed: 8177321]

30. Martinez GR, Loureiro AP, Marques SA, Miyamoto S, Yamaguchi LF, Onuki J, et al. Oxidative and alkylating damage in DNA. Mutat Res 2003;544:115–127. [PubMed: 14644314]

31. Bjelland S, Seeberg E. Mutagenicity, toxicity and repair of DNA base damage induced by oxidation. Mutat Res 2003;531:37–80. [PubMed: 14637246]

32. Cadet J, Douki T, Gasparutto D, Ravanat JL. Oxidative damage to DNA: formation, measurement and biochemical features. Mutat Res 2003;531:5–23. [PubMed: 14637244]

33. Fox ES, Leingang KA. Inhibition of LPS-mediated activation in rat Kupffer cells by N-acetylcysteine occurs subsequent to NF-kappaB translocation and requires protein synthesis. J Leukoc Biol 1998;63:509–514. [PubMed: 9544582]

34. Jaeschke H, Gores GJ, Cederbaum AI, Hinson JA, Pessayre D, Lemasters JJ. Mechanisms of hepatotoxicity. Toxicol Sci 2002;65:166–176. [PubMed: 11812920]

35. Kaplowitz N. Biochemical and cellular mechanisms of toxic liver injury. Sem Liver Dis 2002;22:137–144.

36. Bradham CA, Qian T, Streetz K, Trautwein C, Brenner DA, Lemasters JJ. The mitochondrial permeability transition is required for tumor necrosis factor alpha-mediated apoptosis and cytochrome c release. Mol Cell Biol 1998;18:6353–6364. [PubMed: 9774651]

37. Plumpe J, Malek NP, Bock CT, Rakemann T, Manns MP, Trautwein C. NF-kappaB determines between apoptosis and proliferation in hepatocytes during liver regeneration. Am J Physiol Gastrointest Liver Physiol 2000;278:G173–83. [PubMed: 10644576]

38. Chaisson ML, Brooling JT, Ladiges W, Tsai S, Fausto N. Hepatocyte-specific inhibition of NF-κB leads to apoptosis after TNF treatment, but not after partial hepatectomy. J Clin Invest 2002;110:193–202. [PubMed: 12122111]

39. LaCasse EC, Baird S, Korneluk RG, MacKenzie AE. The inhibitors of apoptosis (IAPs) and their emerging role in cancer. Oncogene 1998;17:3247–3259. [PubMed: 9916987]

40. Baeuerle PA, Henkel T. Function and activation of NF-kB in the immune system. Annu Rev Immunol 1994;12:141–179. [PubMed: 8011280]

41. Flohe L, Brigelius-Flohe R, Saliou C, Traber MG, Packer L. Redox regulation of NF-kappa B activation. Free Radic Biol Med 1997;22:1115–1126. [PubMed: 9034250]

42. Brennan P, O'Neill LA. 2-mercaptoethanol restores the ability of nuclear factor kappa B (NFκB) to bind DNA in nuclear extracts from interleukin 1-treated cells incubated with pyrollidine

dithiocarbamate (PDTC). Evidence for oxidation of glutathione in the mechanism of inhibition of NFκB by PDTC. Biochem J 1996;320:975–981. [PubMed: 9003388]

43. McStay GP, Clarke SJ, Halestrap AP. Role of critical thiol groups on the matrix surface of the adenine nucleotide translocase in the mechanism of the mitochondrial permeability transition pore. Biochem J 2002;367:541–548. [PubMed: 12149099]
44. Heidenreich KA, Kummer JL. Inhibition of p38 mitogen-activated protein kinase by insulin in cultured fetal neurons. J Biol Chem 1996;271:9891–9894. [PubMed: 8626622]
45. Lavoie JN, L'Allemain G, Brunet A, Müller R, Pouyssegur J. Cyclin D1 expression is regulated positively by the p42/44^{MAPK} and negatively by the p38/HOG^{MAPK} pathway of outstanding interest. J Biol Chem 1996;271:20608–20616. [PubMed: 8702807]
46. Ikeda R, Che XF, Ushiyama M, Yamaguchi T, Okumura H, Nakajima Y, et al. 2-Deoxy-d-ribose inhibits hypoxia-induced apoptosis by suppressing the phosphorylation of p38 MAPK. Biochem Biophys Res Commun 2006;342:280–285. [PubMed: 16480951]
47. Naetzker S, Hagen N, Echten-Deckert G. Activation of p38 mitogen-activated protein kinase and partial reactivation of the cell cycle by cis-4-methylsphingosine direct postmitotic neurons towards apoptosis. Genes Cells 2006;11:269–279. [PubMed: 16483315]
48. Ahn EH, Schroeder JJ. Sphinganine causes early activation of JNK and p38 MAPK and inhibition of AKT activation in HT-29 human colon cancer cells. Anticancer Res 2006;26:121–127. [PubMed: 16475687]
49. Sakaida I, Hironaka K, Terai S, Okita K. Gadolinium chloride reverses dimethylnitrosamine (DMN)-induced rat liver fibrosis with increased matrix metalloproteinases (MMPs) of Kupffer cells. Life Sci 2003;72:943–959. [PubMed: 12493575]
50. Sakata N, Patel HR, Terada N, Aruffo A, Johnson GL, Gelfand EW. Selective activation of c-Jun kinase mitogen-activated protein kinase by CD40 on human B cells of special interest. J Biol Chem 1995;270:30823–30828. [PubMed: 8530526]
51. Geerts A, Schellinck P, Bouwens L, Wisse E. Cell population kinetics of Kupffer cells during the onset of fibrosis in rat liver by chronic carbon tetrachloride administration. J Hepatol 1988;6:50–56. [PubMed: 3346533]
52. Shiratori Y, Geerts A, Ichida T, Kawase T, Wisse E. Kupffer cells from CCl4-induced fibrotic livers stimulate proliferation of fat-storing cells. J Hepatol 1986;3:294–303. [PubMed: 3559140]
53. Orfila C, Lepert JC, Alric L, Carrera G, Beraud M, Vinel JP, et al. Expression of TNF-alpha and immunohistochemical distribution of hepatic macrophage surface markers in carbon tetrachloride-induced chronic liver injury in rats. Histochem J 1999;31:677–685. [PubMed: 10576417]
54. Hagens WI, Olinga P, Meijer DK, Groothuis GM, Beljaars L, Poelstra K. Gliotoxin non-selectively induces apoptosis in fibrotic and normal livers. Liver Int 2006;26:232–239. [PubMed: 16448462]
55. Duffield JS, Forbes SJ, Constandinou CM, Clay S, Partolina M, Vuthoori S, et al. Selective depletion of macrophages reveals distinct, opposing roles during liver injury and repair. J Clin Invest 2005;115:56–65. [PubMed: 15630444]

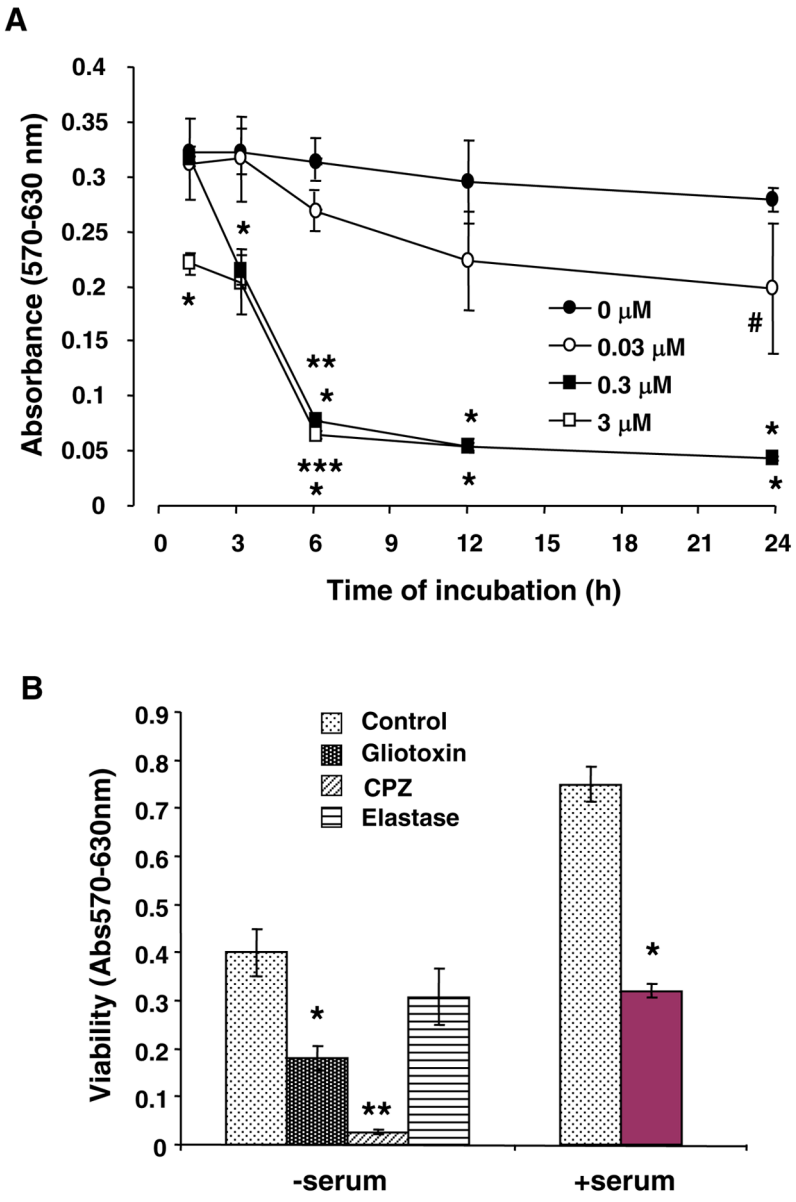

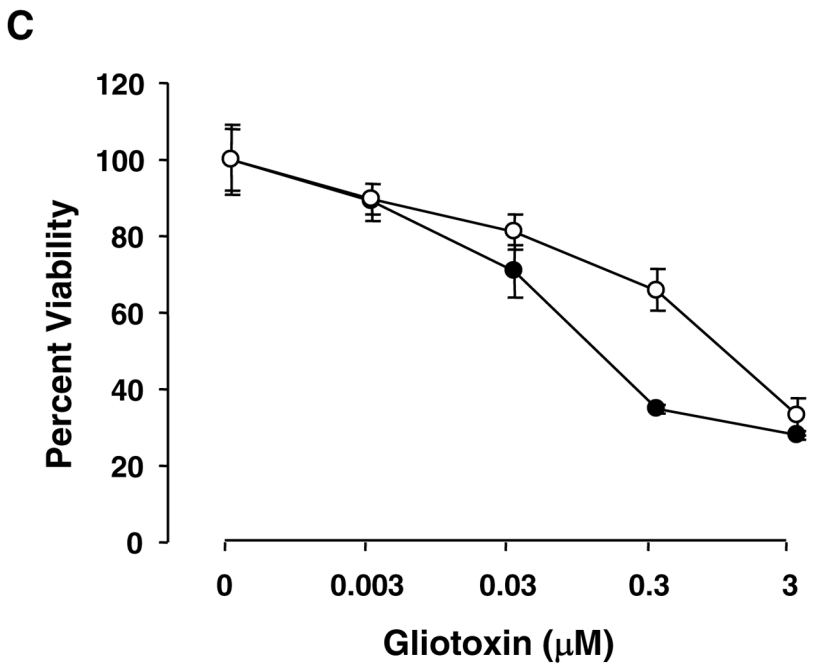

Figure 1.

(A) Time-course and concentration-dependence of gliotoxin-induced decreased viability of Kupffer cells. Cells were washed and placed in serum-free medium containing 0.1% BSA and indicated concentrations of gliotoxin. At specified time points cell viability was determined via MTT (3-(4,5-dimethylthiazol-2-yl)-2,5-diphenyl tetrazolium bromide) assay. #$p<0.05$ vs "0 μM" gliotoxin; *$p<0.001$ vs "0 μM" gliotoxin; **$p<0.001$ vs "3h" gliotoxin; ***$p<0.005$ vs "1 and 3h" gliotoxin. (B) Effect of elastase and chlorpromazine, and of gliotoxin (in the presence of serum). Cells were washed and placed in medium containing 0 or 5% FBS ± 0.3 μM gliotoxin. A set of cells in serum-free medium was incybated in presence of 1 U/ml elastase or 200 μM chlorpromazine. At 3 hours, cell viability was determined via MTT assay. Results show means ± S.D. of triplicate determination. *$p<0.001$ vs control. (C) Comparison of the effect of gliotoxin on Kupffer cells (closed circles) and activated stellate cells (passage 3; open circles) (DNA concentration of 3.61 ± 0.46 and 3.11 ± 0.17 μg/well)demonstrated that the former are more susceptible to its toxic effect at 0.03 ($p<0.05$) and 0.3 μM ($p<0.001$) concentrations. Representative results from 3 separate experiments (each performed in triplicate) are shown.

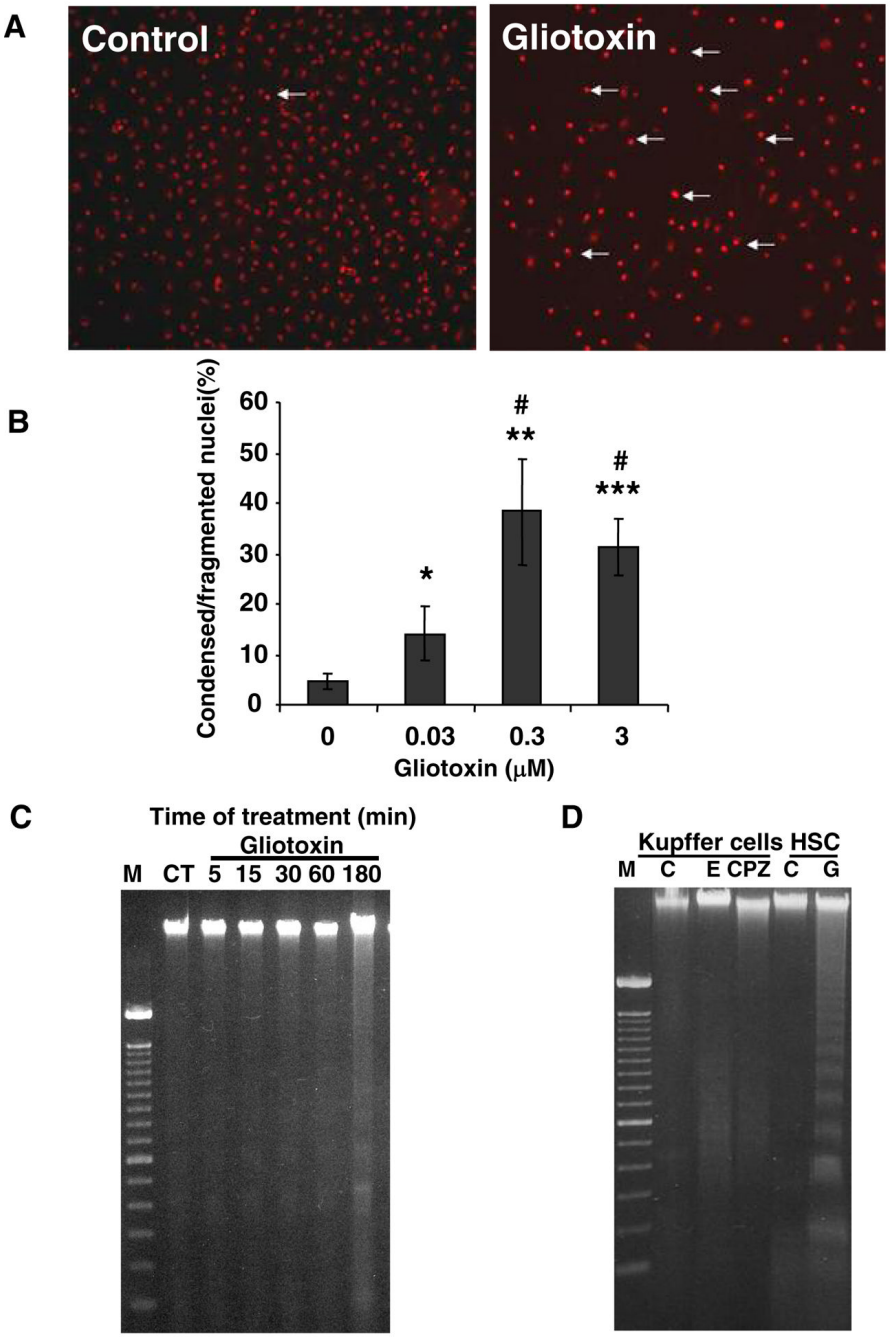

Figure 2. Apoptosis of gliotoxin-challenged Kupffer cells

(A) Cells cultured on glass cover slips were washed and incubated for 3 hours with DMSO (control) or 0.3 μM gliotoxin in serum-free medium. After fixing in paraformaldehyde, the cells were treated with propidium iodide and nuclear morohology was assessed by fluorescent microscopy. Arrows show propidium iodide-stained condensed or fragmented nuclear DNA. (B) Bar graph showing the effect of gliotoxin concentration on the nuclear DNA damage at 3 hours. The values are the percentage of the cells with damaged DNA ± S.D. *, ** and *** $p<0.05$, 0.005 and 0.001 vs "0". #$p<0.05$ vs "0.03 μM" gliotoxin. (C) The cells were treated with 0.3 μM gliotoxin for indicated time periods. Cellular DNA was extracted and electrophoresis was performed to determine fragmentation. CT, control. (D) Kupffer cells were

incubated in serum-free medium without (CT, control) and with 1 U/ml elastase (E) (4 hours) or 200 μM chlorpromazine (CPZ) (1 hour). Activated stellate cells were incubated without (CT, control) or with 0.3 μM gliotoxin (G) for 3 hours. Cellular DNA was extracted and electrophoresis was performed to determine fragmentation. Results shown are representative of 3 separate repetitions using different cell preparations.

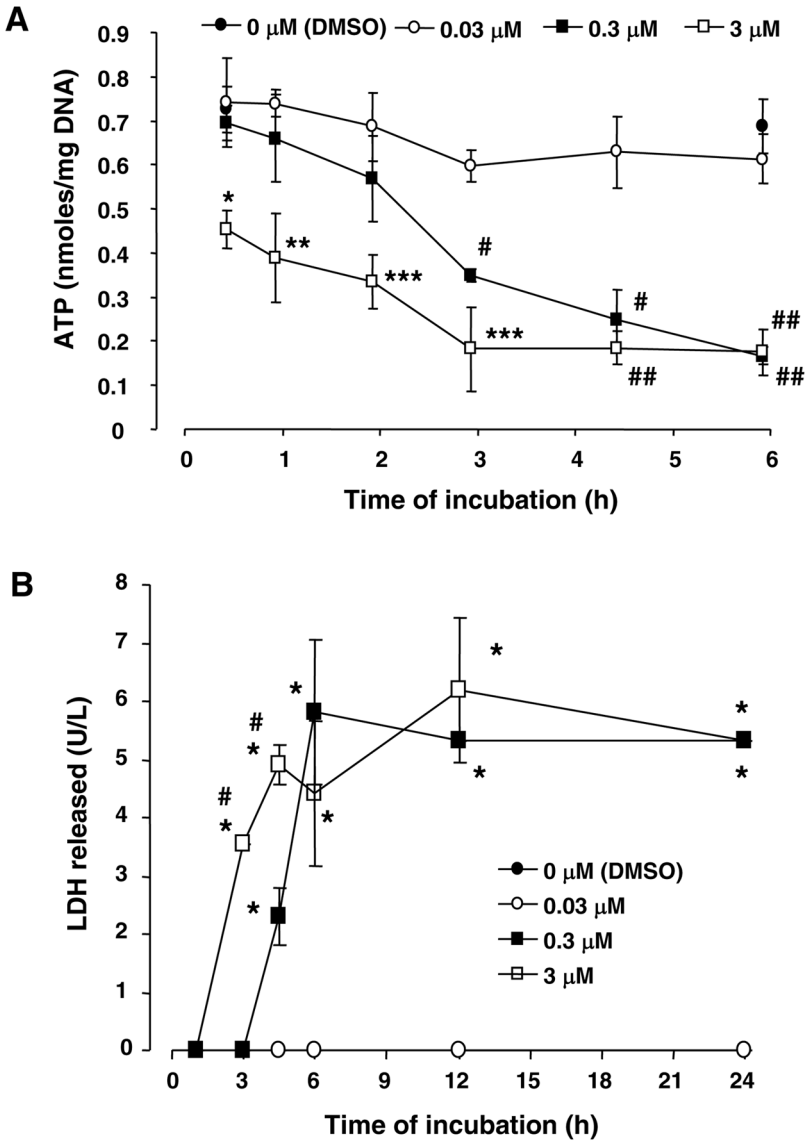

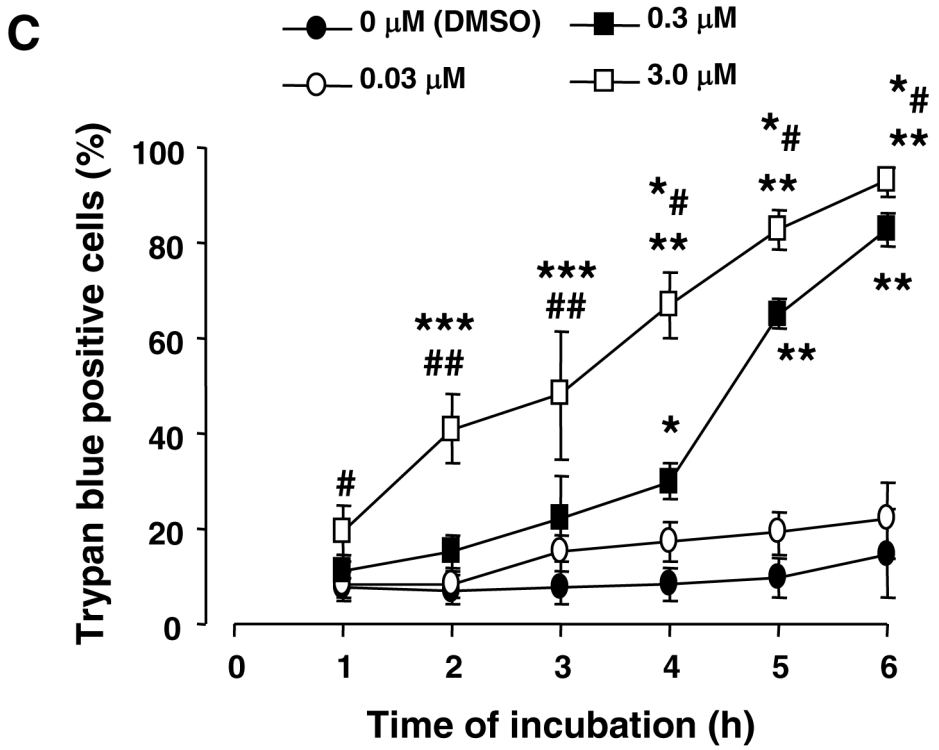

Figure 3. Gliotoxin-induced ATP depletion, extracellular release of lactate dehydrogenase, and trypan blue uptake

(A) Cells were incubated in serum-free medium containing specified concentrations of gliotoxin for indicated time periods. Detached and adhering cells were pooled and ATP concentration was determined. The results show means of triplicate determinations ± S.D. *p<0.01 vs 0 μM gliotoxin and 0.05 vs 0.3 μM gliotoxin; **p<0.025 vs 0 μM gliotoxin and <0.05 vs 0.3 μM gliotoxin; ***p<0.005 vs 0 μM gliotoxin and <0.05 vs 0.3 μM gliotoxin; # and ## p<0.005 and 0.001 vs 0 μM gliotoxin. No significant change in ATP concentration was observed in control (DMSO-treated) and 0.03 μM gliotoxin-treated cells over the experimental time period. (B) Cells were incubated in serum-free medium containing indicated concentrations of gliotoxin. At the specified time intervals the release of lactate dehydrogenase into the medium was determined as described. The results show means of triplicate determinations ± S.D. *p<0.001 vs "0" time; #p<0.001 vs 0.3 μM gliotoxin. (C) The cells were incubated in serum-free medium containing carrier (DMSO) or indicated concentrations of gliotoxin. At 1, 3 and 6 hours trypan blue (final concentration 0.05%) was added and trypan blue-positive and –negative cells were counted. The results show means of triplicate determinations ± S.D. *p<0.01 vs 0 μM gliotoxin; **p<0.001 0 μM gliotoxin; #p<0.05 vs 0 μM gliotoxin; ##p<0.025 vs 0 μM gliotoxin; ***p<0.05 vs 0.3 μM gliotoxin; *#p <0.01 vs 0.3 μM gliotoxin. All experiments were repeated at least 3 times using different cell preparations with essentially similar results.

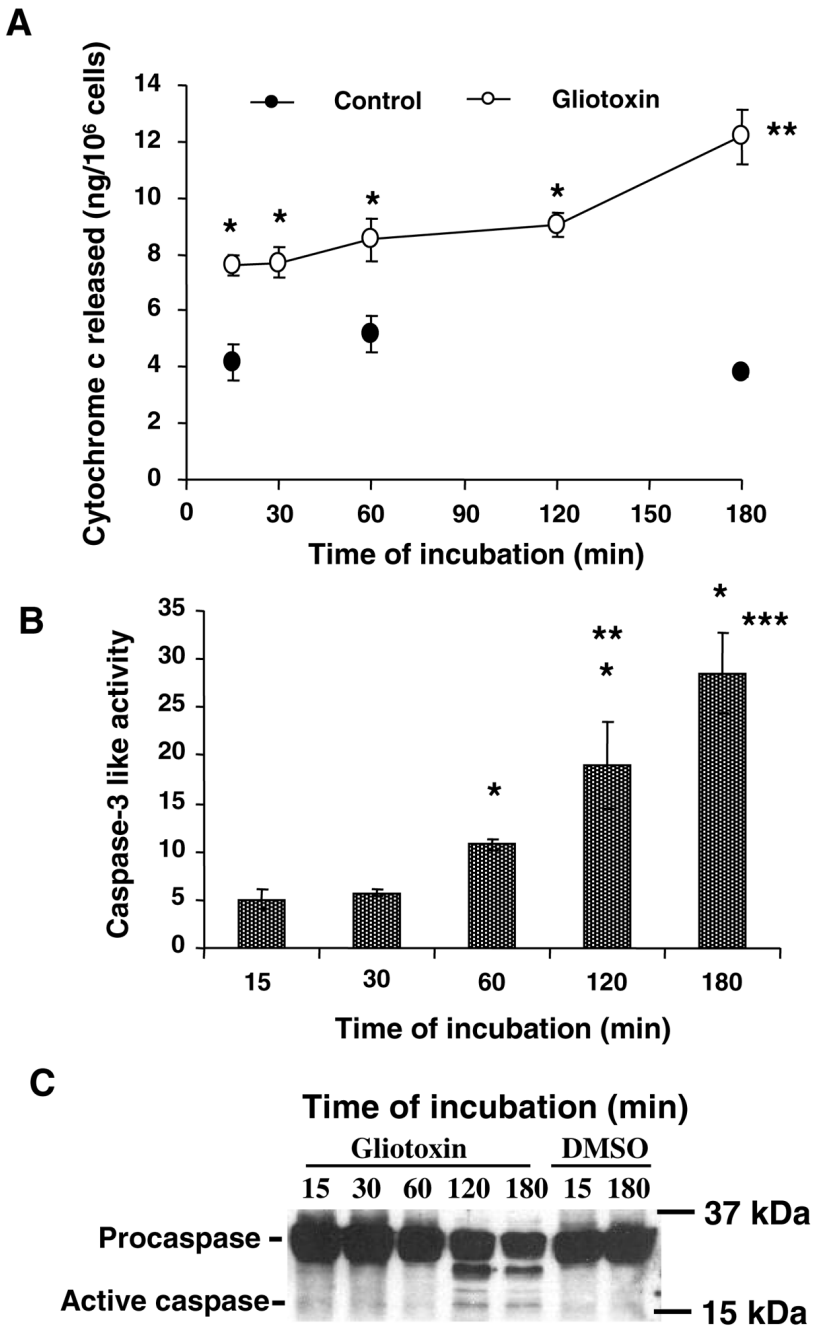

Figure 4. Mitochondrial cytochrome c release and caspase-3 activation in gliotoxin-treated Kupffer cells

Kupffer cells were incubated in serum-free medium with 0.3 μM gliotoxin or DMSO for indicated time points. (A) Cytosolic cytochrome c at various times. *p<0.005 vs 0 μM gliotoxin; **p<0.05 vs 2 h with gliotoxin. (B) Caspase-3-like activity in the vehicle or gliotoxin-treated cells was determined as described in the Methods section. The results are expressed as caspase-3-like activity relative to control using the formula [ΔFU (stimulated-unstimulated cells)/slope], where FU are fluorescence units due to release of bound 7-amino-4-trifluoromethyl cumarin (AFC) from the conjugate with caspase substrated DEVD-fmk. Standard curve was developed using 0–4 μM AFC. *p<0.005 vs 15/30 min; **p<0.05 vs 1 h;

***$p<0.01$ vs 1 h. (C) Cellular proteins were extracted for determination of caspase-3 activation via Western analysis. Results in experiments of A and B are means of triplicate determinations ± S.D. from 3 separate experiments, while results in C show a representative blot of 3 experiments.

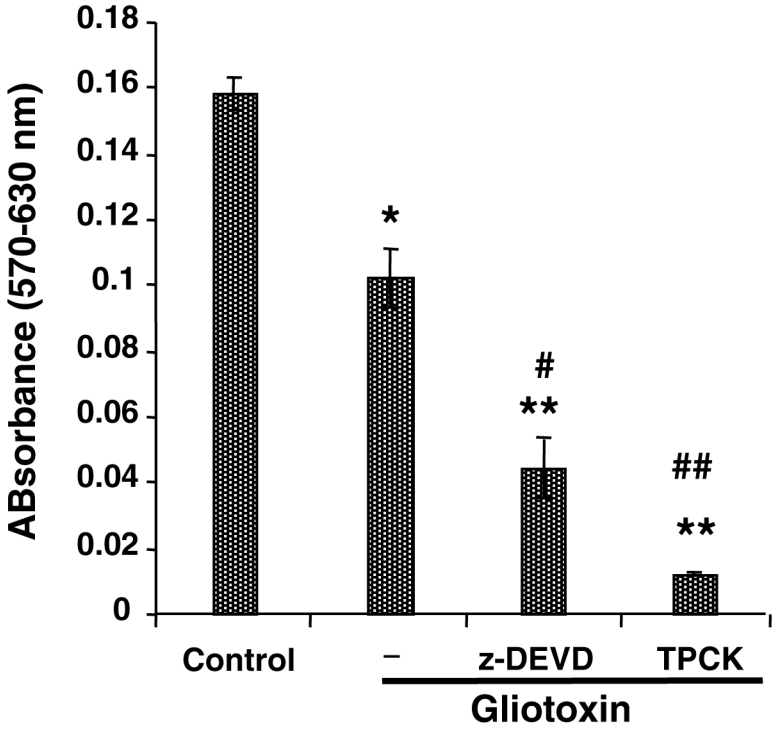

Figure 5. Effect of caspase and serine protease inhibitors on gliotoxin-stimulated Kupffer cells

Cells were preincubated for 30 min with 5 μM Z-DEVD.FMK or 10 μM TPCK prior to addition of 0.3 μM gliotoxin. Cell viability was determined by MTT assay at 3 hours. Results are means ± S.D. of triplicate determinations ± S.D. from 3 separate experiments. *$p<0.005$ vs control; **$p<0.001$ vs control; #$p<0.005$ vs gliotoxin; ##$p<0.001$ vs gliotoxin. No nonspecific effect of the inhibitors was observed on Kupffer cell viability (results not shown).

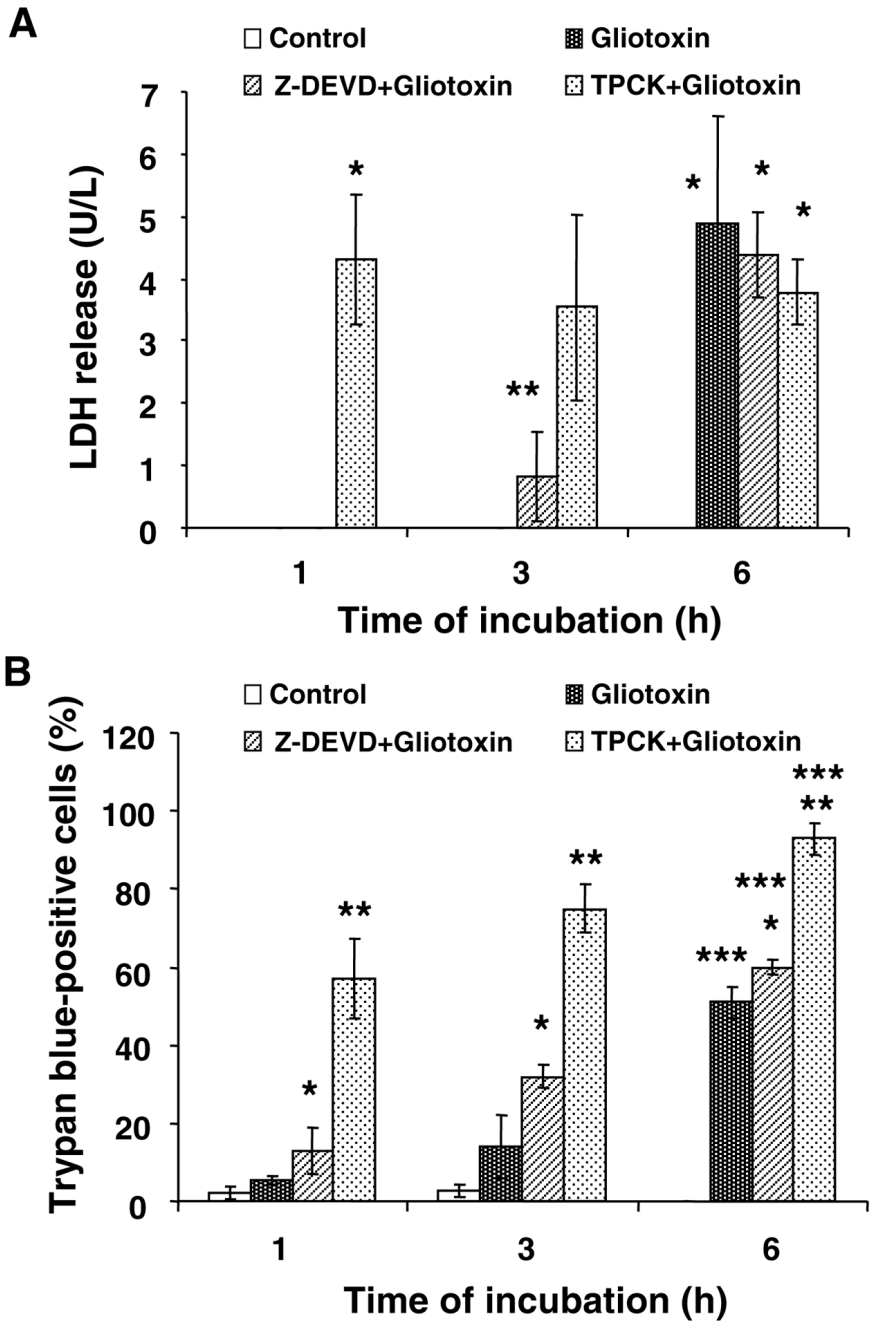

Figure 6. Exacerbation of gliotoxin-induced death of Z-DEVD.fmk- and TPCK-pretreated Kupffer cells

Cells were washed and incubated with 5 μM Z-DEVD.fmk or 10 μM TPCK for 30 minutes prior to addition of 0.3 μM gliotoxin. At the indicated time points LDH release (A) and trypan blue uptake were determined as described in the Methods section. Results are means ± S.D. of triplicate determinations ± S.D. from 3 separate experiments. (A) *$p<0.001$ vs control; **$p<0.05$ vs control. (B) *$p<0.05$ vs gliotoxin; **$p<0.001$ vs control or 0.005 vs gliotoxin; ***$p<0.001$ vs control.

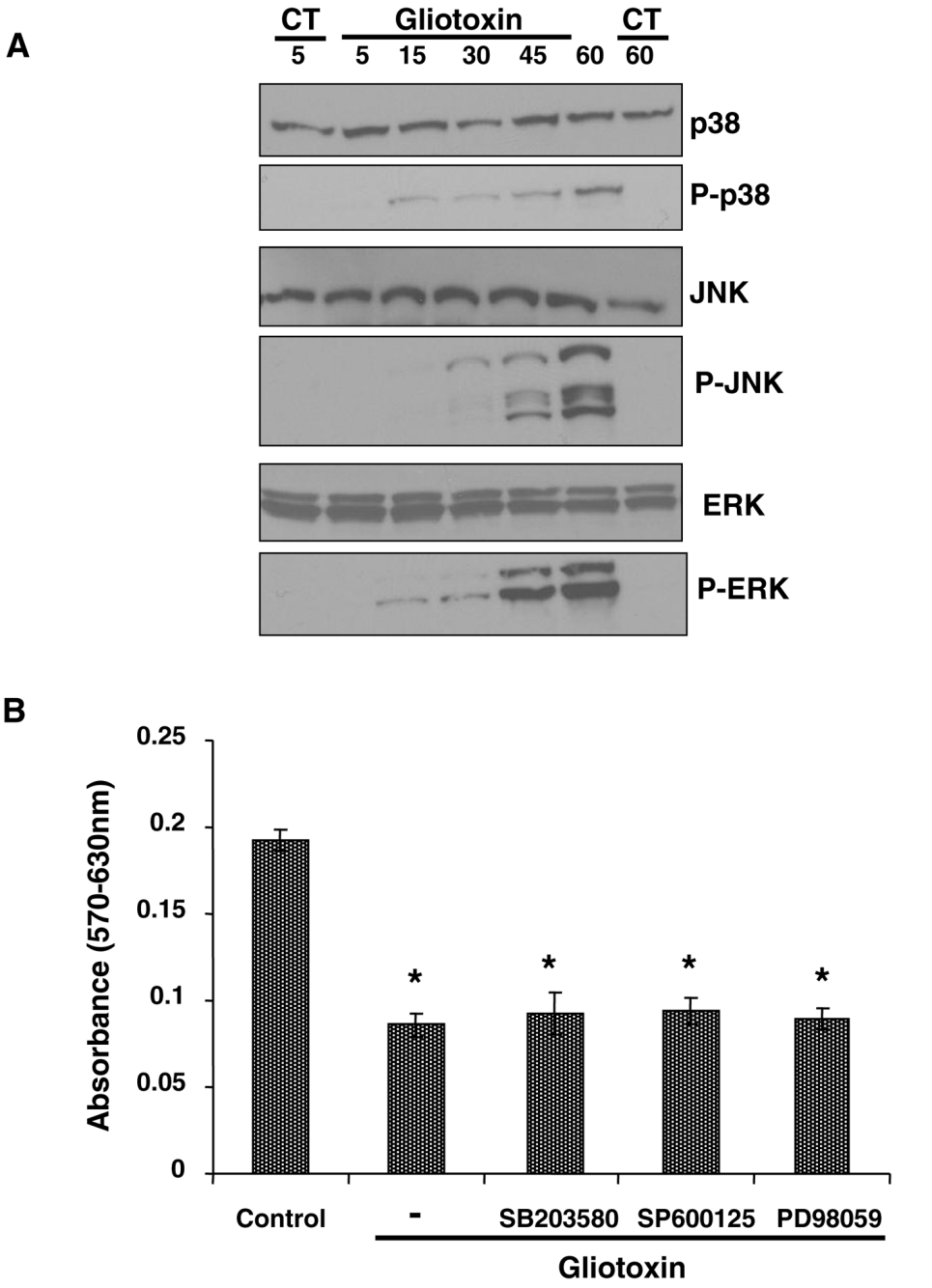

Figure 7. Activation of MAPKs by gliotoxin

(A) Cells were treated with 0.3 μM gliotoxin for indicated time periods. For control (CT), cells were incubated with vehicle (DMSO) for 5 and 60 min. Phosphorylation of p38, JNK and ERK1/2 was determined by Western analysis as described in the Methods section. No change in the phophorylation was observed in the control cells over the experimental time period. Western blot shown is a representative of 2 separate experiments. (B) Cells were pretreated with specific MAPK inhibitors SB203580 (10 μM; p38 kinase), PD98059 (10 μM; ERK1/2 kinase), SP600125 (10 μM; JNK kinase) and PDTC (50 μM; NFκB) for 30 min, and then challenged with 0.3 μM gliotoxin. Cell viability was determined at 3 hours. The results show means of triplicate determinations ± S.D. of triplicate determinations from 3 separate

experiments. *p<0.001 vs control. These inhibitors, at the concentrations used, did not affect Kupffer cell viability on their own (results not shown).

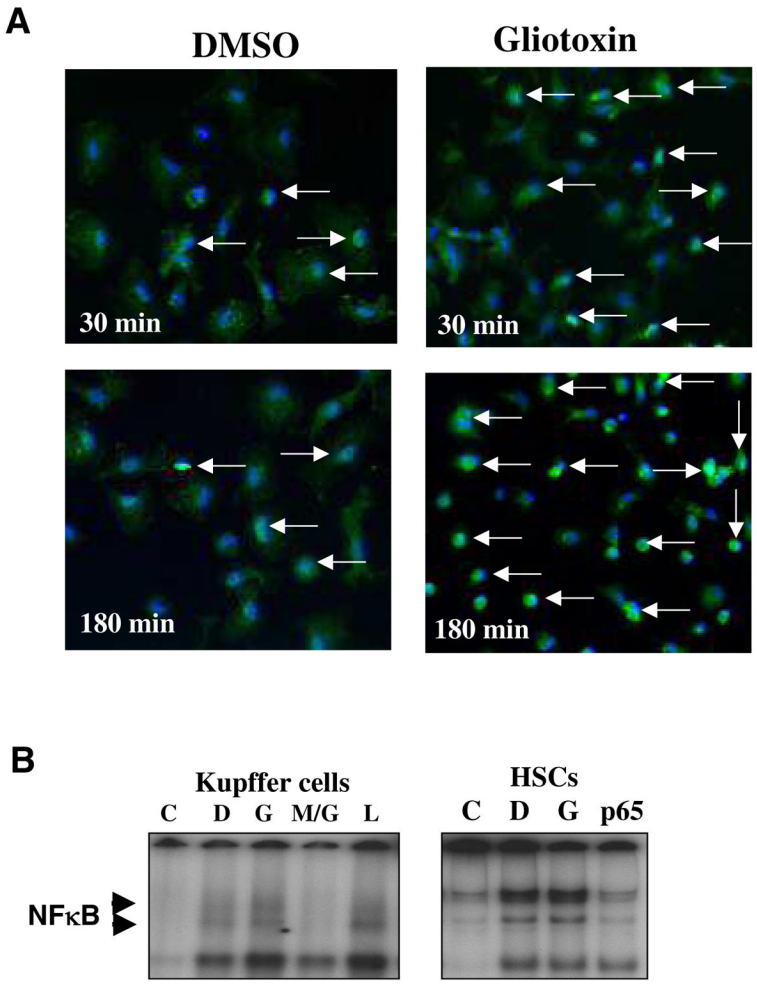

Figure 8. Effect of gliotoxin on NFκB nuclear translocation

(A) Cells were washed and challenged with 0.3 μM gliotoxin or DMSO vehicle. Immunostaining for p65-NFκB was performed as described in the Methods section. In DMSO-treated cells, p65-NFκB is mostly localized to the cytoplasm, while its nuclear translocation is increased upon treatment with gliotoxin (arrows). (B) Gel shift assay. The nuclear fractions from DMSO, 0.3 μM gliotoxin or 0.1 μg/ml LPS-treated cells (1 hour) were used to determine translocation of NFκB. Preincubation for 10 min with an inhibitor of NFκB translocation (MG132; 10 μg/ml) was employed to assess stimulation by gliotoxin. C, competition with 100-fold molar excess of cold probe; D, DMSO control; G, gliotoxin; M/G, MG132 + gliotoxin; L, LPS. Gel on the right shows no difference in nuclear NFκB in activated HSC treated without (DMSO vehicle-D) and with gliotoxin (G) for one hour; these data are consistent with that reported by Wright et al (1).C, excess cold probe; p65, preincubation of nuclear extract with 1 μg of p65 antibody recognizing NFκB subunit. The experiments were repeated twice with similar results.

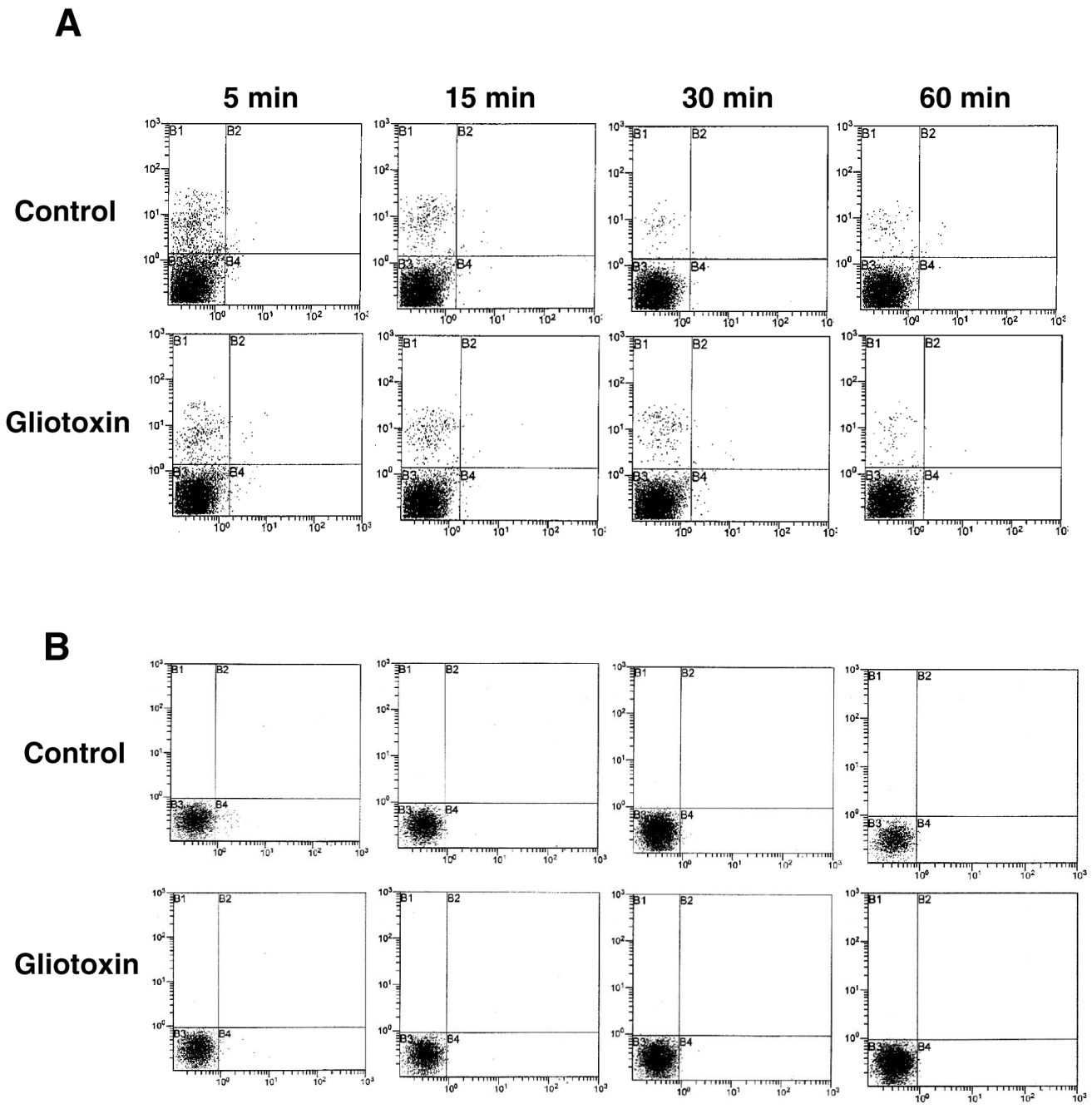

Figure 9. Reactive oxygen species in gliotoxin-stimulated cells

Cells were washed and loaded with (A) hydroethidine (HE) or (B) dihydro-2′,7′-dichlorofluorescein diacetate (DCFH-DA) respectively (both at 10 μM final concentration) in serum-free DMEM without phenol red for 30 min at 37°C and challenged with 0.3 μM gliotoxin for indicated time periods. The cells were then processed for SO (A) and H_2O_2 (B) determination by flow cytometry. X axis represents hydroethidine or DCF fluorescence, and Y axis represents number of events. The results shown are from a representative experiment repeated two times.

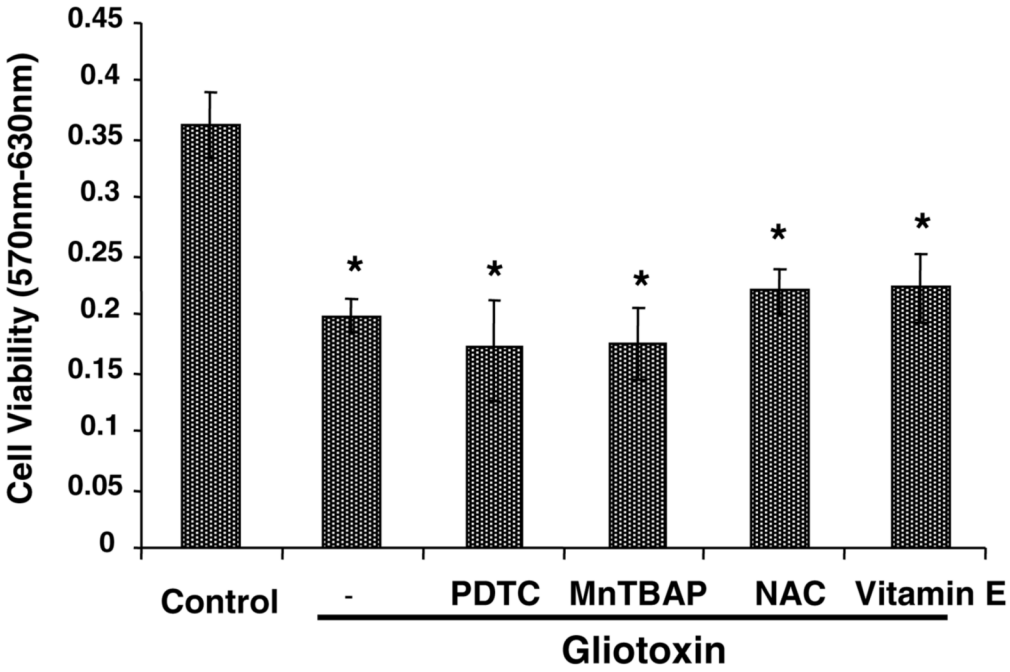

Figure 10. Effect of antioxidants on gliotoxin-induced loss of viability

Cells were preincubated with 50 μM PDTC, 100 μM vitamin E, 20 μM Mn-TBAP or 250 μM N-acetylcysteine for 30 min prior to the addition of 0.3 μM gliotoxin. Control cells were incubated with equivalent volume of carrier DMSO. After 3 hours of incubation, viability was determined by MTT assay. The results show means of triplicate determinations ± S.D. *$p<0.005$ vs control. The results shown are from a representative experiment repeated two times.

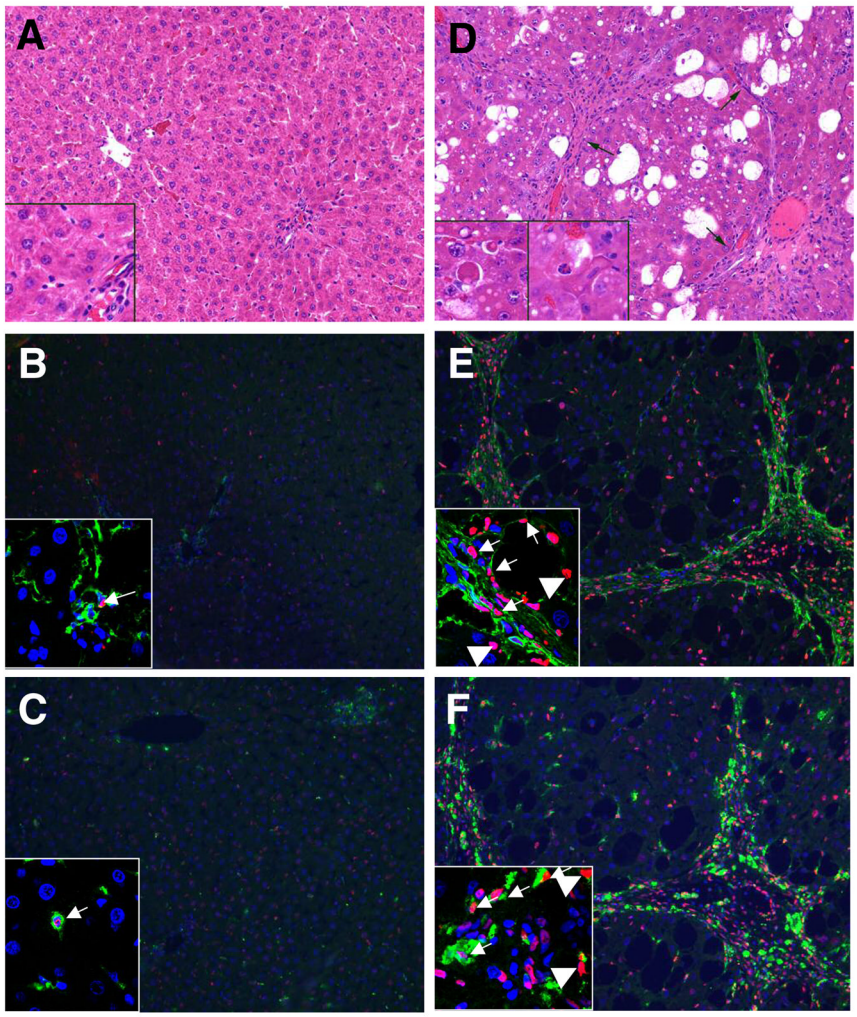

Figure 11. Effect of gliotoxin on hepatic cells *in vivo*

Cirrhosis was induced in rats by treatment with CCl_4 as described in the Methods section. Control rats received vehicle (peanut oil). Gliotoxin (3 mg/kg) was injected intraperitoneally, and 6 hours later the livers were harvested and processed for the determination of apoptotic cells. Top panel: (A) Gliotoxin treated control rat: This survey photomicrograph (10x H&E) shows normal architecture with a terminal hepatic venule on the left and portal tract on the right half of the image. Hepatocytes are the predominant cell population and are of uniform size without evidence of apoptotic activity. Inset (40X, lower left) shows unremarkable hepatocytes. Several sinusoidal cells are also seen, and a portion of portal tract is present in the lower right hand corner. (D) Cirrhotic rat treated with gliotoxin: This low power photomicrograph (10x H&E) shows severe architectural distortion due to the presence of fibrous bands forming complete and incomplete nodules. A representative nodule is shown (arrows). Hepatocytes show variable degrees of cytoplasmic vacuolization. A markedly expanded subset of cells is also present. Insets (40x, lower left) show individual apoptotic hepatocytes (“Councilman bodies”) in this liver. The leftmost inset shows two well developed apoptotic cells with eosinophilic cytoplasm, consistent with hepatocytes. The right hand inset shows an early apoptotic cell clearly identifiable as a hepatocyte. Chromatin disintegration is apparent in comparison to surrounding hepatocyte nuclei. Middle and bottom panels show respectively desmin + TUNEL (B,E) and ED-2 + TUNEL (C, F) co-stained liver sections of gliotoxin-treated control (B, C) and cirrhotic rats (E, F) (magnification x20). Several TUNEL-

positive Kupffer cells, stellate cells and hepatocytes can be seen. Insets are the confocal images (magnification X60) showing apoptotic cells; thin arrows- stellate or Kupffer cells; thick arrows- hepatocytes. For each condition 4 control and 5 cirrhotic rats were used. Green colour represents ED-2 or desmin staining and red represents TUNEL staining.

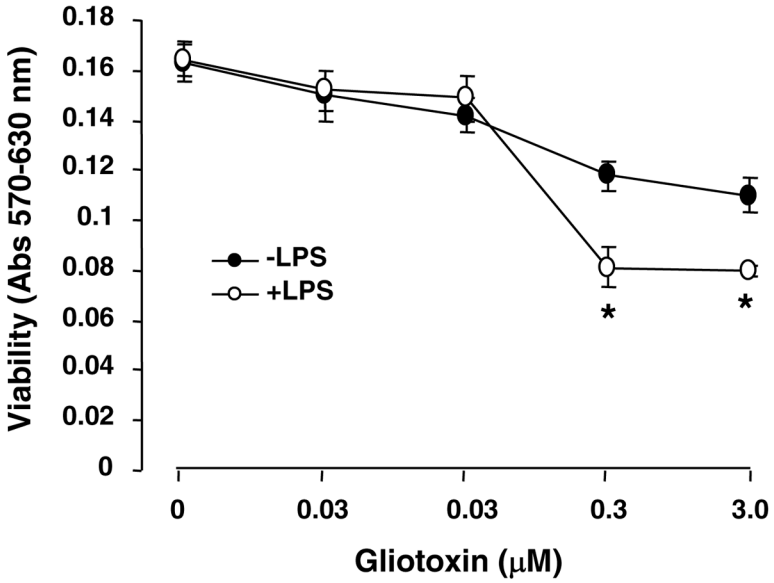

Figure 12. Effect of *in vitro* activation of Kupffer cells on gliotoxin-induced death

The cells were preincubated with 0.1 μg/ml LPS in 0.1% serum-containing medium for 1 hour for activation (33). The medium was then replaced with serum-free medium containing 0–3.0 μM gliotoxin and at cell viability was determined at 3 hours. *$p<0.01$ vs incubation without LPS. The results shown are from a representative experiment repeated two times.